Environmental Science & Technology

pubs.acs.org/est

Article

# Natural and Anthropogenically Influenced Isoprene Oxidation in Southeastern United States and Central Amazon

Lindsay D. Yee,* Gabriel Isaacman-VanWertz, Rebecca A. Wernis, Nathan M. Kreisberg, Marianne Glasius, Matthieu Riva, Jason D. Surratt, Suzane S. de Sá, Scot T. Martin, M. Lizabeth Alexander, Brett. B. Palm, Weiwei Hu, Pedro Campuzano-Jost, Douglas A. Day, Jose L. Jimenez, Yingjun Liu, Pawel K. Misztal, Paulo Artaxo, Juarez Viegas, Antonio Manzi, Rodrigo A. F. de Souza, Eric S. Edgerton, Karsten Baumann, and Allen H. Goldstein*

Cite This: *Environ. Sci. Technol.* 2020, 54, 5980−5991

Read Online

ACCESS | Metrics & More | Article Recommendations | Supporting Information

**ABSTRACT:** Anthropogenic emissions alter secondary organic aerosol (SOA) formation chemistry from naturally emitted isoprene. We use correlations of tracers and tracer ratios to provide new perspectives on sulfate, $NO_x$, and particle acidity influencing isoprene-derived SOA in two isoprene-rich forested environments representing clean to polluted conditions—wet and dry seasons in central Amazonia and Southeastern U.S. summer. We used a semivolatile thermal desorption aerosol gas chromatograph (SV-TAG) and filter samplers to measure SOA tracers indicative of isoprene/$HO_2$ (2-methyltetrols, $C_5$-alkene triols, 2-methyltetrol organosulfates) and isoprene/$NO_x$ (2-methylglyceric acid, 2-methylglyceric acid organosulfate) pathways. Summed concentrations of these tracers correlated with particulate sulfate spanning three orders of magnitude, suggesting that 1 $\mu g\ m^{-3}$ reduction in sulfate corresponds with at least ∼0.5 $\mu g\ m^{-3}$ reduction in isoprene-derived SOA. We also find that isoprene/$NO_x$ pathway SOA mass primarily comprises organosulfates, ∼97% in the Amazon and ∼55% in Southeastern United States. We infer under natural conditions in high isoprene emission regions that preindustrial aerosol sulfate was almost exclusively isoprene-derived organosulfates, which are traditionally thought of as representative of an anthropogenic influence. We further report the first field observations showing that particle acidity correlates positively with 2-methylglyceric acid partitioning to the gas phase and negatively with the ratio of 2-methyltetrols to $C_5$-alkene triols.

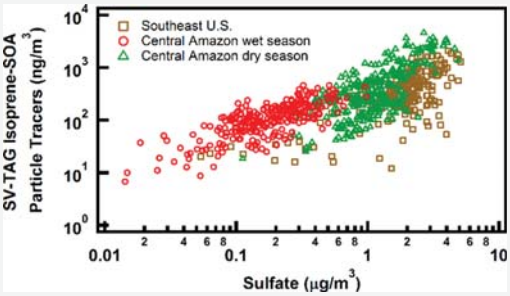




## 1. INTRODUCTION

Isoprene-derived carbon contributes significantly to the global secondary organic aerosol (SOA) budget.[1] As such, it contributes to global impacts of SOA including air quality, adverse human health effects, and affecting Earth's radiative balance. SOA formed from oxidation of biogenic volatile organic compounds (VOCs), such as isoprene, is enhanced by anthropogenic pollutants including $NO_x$, $SO_2$, $O_3$, black carbon, and particulate matter.[2−7] Still, atmospheric measurements constraining chemical mechanisms and understanding of the extent by which these chemical levers affect isoprene-derived SOA formation are limited.[8−14] The anthropogenic impact of $NO_x$ and $SO_2$ (as a precursor to particulate sulfate) on SOA formation from isoprene has been investigated extensively in the laboratory.[2,3,15−20] $NO_x$ ultimately controls the branching ratio between different chemical pathways to SOA derived from isoprene (referenced hereafter as isoprene-SOA), and particulate sulfate facilitates the reactive uptake of isoprene-derived gas-phase intermediates.[5,21−23] Sulfate also affects particle liquid water content and particle pH, all of which affect the physicochemical conditions under which isoprene-SOA forms.[8,24−29]

Isoprene reacts primarily with OH radicals during daytime forming an isoprene peroxy radical. At sufficiently low $NO_x$ levels (referenced as isoprene/$HO_2$ pathway), an isoprene hydroperoxide (ISOPOOH) is formed, and subsequent oxidation of ISOPOOH with an OH radical results in rearrangement to gas-phase isoprene epoxydiol (IEPOX) isomers.[30] Under these conditions, isoprene-SOA derives primarily from acid-catalyzed multiphase chemistry of IEPOX involving uptake into the aqueous phase of particulate matter,[21,22,27,30−33] and this SOA is referred to as IEPOX-SOA. IEPOX-SOA is estimated to contribute up to 30% of the OA across many sites worldwide.[7,34,58] Several molecular

Received: February 8, 2020
Revised: April 7, 2020
Accepted: April 9, 2020
Published: April 9, 2020




https://dx.doi.org/10.1021/acs.est.0c00805
*Environ. Sci. Technol.* 2020, 54, 5980−5991

tracers of IEPOX-SOA previously measured in the laboratory/field include 2-methyltetrols and their oligomers,[21,35−37] $C_5$-alkene triols,[15,16,38,39] methyl tetrahydrofurans, and methyltetrol sulfates.[5,21,24,40−42] These molecular tracers (all isomers listed Table S2) will be referred to in the rest of this paper as 2-MTs, C5ALKTRIOLS, THFs, and MT-OSs, respectively. Oligomers formed from some of these tracers have been observed,[15] although their mass contribution remains unconstrained, and they may decompose during thermal desorption analysis contributing to the observed tracers.[42−45]

The presence of higher levels of $NO_x$ (referenced as isoprene/$NO_x$ pathway) leads to a parallel route of SOA formation from oxidation of methacrolein (MACR),[17,21,46] referred to here as MACR-SOA. Oxidation of MACR forms methacryloyl peroxynitrate (MPAN), which further oxidizes to methacrylic epoxide (MAE)[47] and hydroxy methyl methyl lactone (HMML).[48] Multiphase chemistry of MAE/HMML leads to 2-methylglyceric acid (2-MG), 2-methylglyceric acid organosulfate (2-MG-OS), and their respective oligomeric forms.[15,49,50] This route is typically less efficient in SOA formation compared to the IEPOX-SOA route because MPAN survival in the atmosphere is strongly enhanced at lower temperatures while isoprene emissions increase exponentially with temperature. Thus, reaction with OH must occur on a timescale competitive to MPAN decomposition to sufficiently form MACR-SOA intermediates.[51]

Field observations spanning clean to polluted conditions are sparse[36] but important for examining correlations between molecular markers of isoprene-SOA and chemical levers on OA chemistry (e.g., $NO_x$, particulate sulfate, and particle pH). Here, we made measurements in two similar though unique environments (Southeastern United States and central Amazon) to examine isoprene chemistry under such atmospheric conditions. Each region is high in isoprene emissions yet with differing histories and trajectories of anthropogenic influence. Previous measurements in another region of the Amazon Basin (Rondônia, Brazil) included offline filter-based measurement of isoprene/$HO_x$ tracers, 2-MTs and C5ALKTRIOLS.[36] Here we report in situ measurement of these tracers in addition to isoprene/$NO_x$ tracer 2-MG in both gas and particle phases, as well as offline filter-based measurements of isoprene-derived organosulfates, MT-OSs and 2-MG-OS. Through correlation analyses utilizing this newly available higher time resolution tracer and particle composition data, we further specify the role of particle acidity and the extent by which anthropogenically and naturally derived $NO_x$ and sulfate promote their formation, affect tracer ratios, and determine their gas/particle partitioning.

## 2. MATERIALS AND METHODS

This work relies primarily on data collected using a semivolatile thermal desorption aerosol gas chromatograph (SV-TAG) and a suite of supporting instrumentation at two field sites over three campaigns. Measurements were conducted at the Centreville, Alabama, U.S.A. site during the Southern Oxidant and Aerosol Study 2013 (SOAS)[52] and the downwind of Manaus, Brazil "T3" site during the Green Ocean Amazon (GoAmazon 2014/5) field campaigns.[53,54] SOAS took place from 1 Jun 2013 to 15 Jul 2013. For GoAmazon 2014/5, measurements reported herein took place from 1 Feb to 26 Mar 2014, known as the first intensive operating period 1 (IOP1) and referred to hereafter as the "wet season", and from 15 Aug to 15 Oct 2014, known as IOP2 and referred to hereafter as the "dry season." Both sites represent areas of high isoprene emissions affected by urban centers (i.e., Birmingham, Alabama, for Centreville and Manaus, Amazonas for "T3"). Manaus plume impacted sampled air masses at "T3" ∼40% (wet season) and ∼60% (dry season) of the time. The dry season is further characterized by an enhancement in regional biomass burning influences.[54,55]

SV-TAG provided gas and particle phase speciation of semivolatile organic compounds, an aerodyne aerosol mass spectrometry (AMS) provided $PM_1$ organic and inorganic speciation, and quartz filter analysis provided speciation of OSs in $PM_{2.5}$ samples collected during SOAS and $PM_1$ filter samples collected during GoAmazon. An Ionicon proton transfer reaction mass spectrometer (PTRMS) was used to measure the gas-phase concentrations of isoprene. Instrument operation, analysis, and deployment details during these field campaigns were published for SV-TAG,[43,56,57] AMS,[13,58,59] particulate filter collection and OSs analysis by liquid chromatography coupled to electrospray ionization high-resolution mass spectrometry (LC/ESI-HR-MS),[14,57,60,61] and PTRMS.[62,63] Synthesized MT-OSs were analyzed by SV-TAG to estimate the degree of their decomposition during analysis; roughly <10% of the measured 2-MTs and C5ALKTRIOLs are formed through decomposition of MT-OSs (for details, see the Supporting Information). Model results for particle pH and liquid water content (LWC) are the same as used by Isaacman-VanWertz et al.,[43] utilizing the thermodynamic model ISORROPIA-II.[64] During SOAS, meteorological data (temperature, relative humidity, wind direction) and concentrations of $NO_x$, $NO_y$, and $O_3$ were measured within the SouthEastern Aersol Research and Characterization Network (SEARCH).[65] During GoAmazon, these parameters were measured within the co-located U.S. Department of Energy Atmospheric Radiation Measurement Climate Facility comprising Atmospheric Radiation Measurement Facility One (AMF-1) and Mobile Aerosol Observation System (MAOS).[66]

## 3. RESULTS AND DISCUSSION

**3.1. Field Campaign Comparisons.** Concentration ranges from the GoAmazon wet/dry season and SOAS for isoprene, $PM_1$ organic, sulfate, and daytime $NO_y$ (representative of photochemical conditions and processed $NO_x$) are summarized (Figure S1). GoAmazon wet season median concentrations are the lowest, representing the least polluted and lowest aerosol loading conditions although median $NO_y$ was only slightly lower with a similar range to other measurement campaigns. The GoAmazon dry season is characterized with higher biogenic emissions, regional biomass burning emissions, and less wet deposition,[55] having the highest $PM_1$ organic although between the wet season and SOAS for isoprene and sulfate. SOAS exhibits the highest anthropogenic influence (sulfate) and the highest isoprene concentrations. The median $NO_y$ concentration during SOAS is slightly higher than those of the other campaigns, although narrow in range, suggesting fewer large local emission sources and a more regionally averaged contribution sampled in this rural region of Alabama. The greater range of observed $NO_y$ values during GoAmazon reflects pollution plumes influencing local chemistry.[67] We note that while more polluted on average than GoAmazon, SOAS pollution levels were in fact the lowest since measurements began in 1999 for that region.[68] Mean temperature ($T$) and relative humidity (RH) during


https://dx.doi.org/10.1021/acs.est.0c00805
Environ. Sci. Technol. 2020, 54, 5980−5991

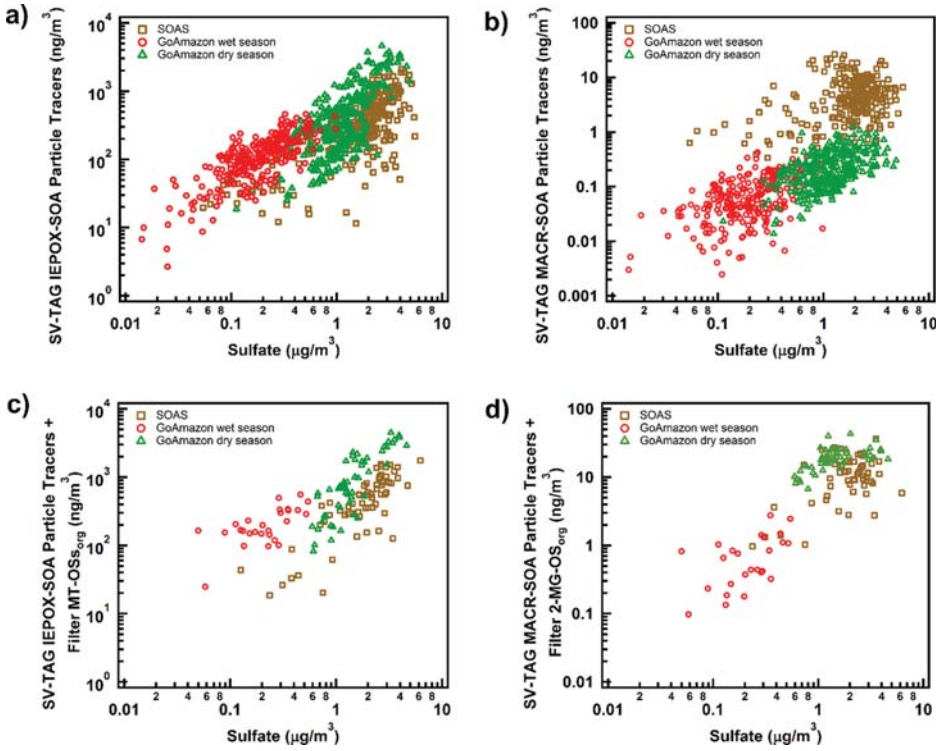


**Figure 1.** Particle-phase tracers from (a) IEPOX and (b) MACR channels of isoprene-SOA formation as measured by SV-TAG and associated particulate sulfate as measured by AMS during SOAS (brown squares), the GoAmazon wet season (red circles), and the GoAmazon dry season (green triangles). Coefficients of determination, $R^2$ = 0.48, 0.49, 0.57, and 0.40 for SOAS, the GoAmazon wet season, the GoAmazon dry season, all data sets, respectively, for (a) IEPOX-SOA tracers correlated with sulfate. $R^2$ < 0.25 for each individual data set and all data sets taken together for (b) MACR-SOA tracers correlated with sulfate. Summation of (c) SV-TAG IEPOX-SOA particle-phase tracers and filter MT-OSs organic and (d) SV-TAG MACR-SOA particle-phase tracers and filter 2-MG-OS organic.

corresponding measurement times were as follows: SOAS $T_{mean}$ = 24.7 °C, $RH_{mean}$ = 82%; GoAmazon wet season $T_{mean}$ = 26.5 °C, $RH_{mean}$ = 90%; GoAmazon dry season $T_{mean}$ = 27.9 °C, $RH_{mean}$ = 83%.[43]

**3.2. Tracer Correlations Revealing Chemical Factors Influencing Isoprene Chemistry.** The range of conditions for biogenic and anthropogenic emissions observed in these campaigns provides a useful opportunity to compare the chemical fate of isoprene during oxidation under clean versus polluted conditions. Temporal variability in SV-TAG-measured molecular markers (particle-only and gas + particles) was compared with each other and several other calculated/measured parameters through correlation analyses. Coefficients of determination, $R^2$, are summarized in Table S3 for SOAS, GoAmazon wet season, GoAmazon dry season, all data sets taken together. Many moderate correlations ($R^2 \geq 0.4$, values bolded in Table S3) between measured tracers and organic, sulfate, nitrate, and ozone concentrations within any one deployment period exist. When measurements from SOAS and both GoAmazon deployments are taken together, correlations for IEPOX-SOA tracers are still clearly the strongest with sulfate ($R^2$ = 0.40). Taken individually, correlations of molecular markers of IEPOX-derived SOA tracers (i.e., 2-MTs, C5ALKTRIOLS) with sulfate during GoAmazon are generally higher than previous analyses for other sites throughout the United States.[10,11] This could derive from the following: (1) owing to hourly measurements by SV-TAG, increased time resolution may better capture the dynamics of particle composition; and (2) a wide range in sulfate concentrations was measured across these deployments, revealing that correlation with sulfate is strong across the whole range from polluted to extremely clean conditions, not just when anthropogenic pollution is abundant. Correlations of tracers with particle pH and liquid water content (LWC) vary across different deployments from nonexistent to moderate, and we further discuss these relationships in the context of isoprene-SOA formation.

*3.2.1. Influence of Sulfate on Isoprene-SOA from Clean to Polluted Conditions.* Many studies interpret enhancements in isoprene-SOA formation correlated with sulfate as an indicator of isoprene-SOA formation enhanced by anthropogenically derived sulfate.[2,9,10,69] Sulfate is cited as having a central role in influencing SOA formation from isoprene by enhancing uptake of IEPOX/MAE/HMML into the particle phase by affecting particle surface area[69] as well as hygroscopicity, thereby affecting the LWC, aqueous particle volume,[12,29,70,71] and particle acidity.[21,24,27,47] It can also facilitate "salting in" conditions to enhance IEPOX uptake into the particle phase and directly reacts with epoxide intermediates to form organosulfates,[5,47] whereas the free acid form (sulfuric acid) serves as a catalyst in the hydrolysis of IEPOX to form 2-MTs.[9,33] It was surmised that sulfate is the limiting reagent in isoprene-SOA formation in the Southeastern United States based on significant correlation between sulfate and estimated isoprene-derived SOA (positive matrix factorization analysis of AMS mass spectra).[9,34] While yields of several isoprene SOA molecular markers increase in the presence of particulate sulfate in acidic particles, atmospheric measurements reporting


https://dx.doi.org/10.1021/acs.est.0c00805
Environ. Sci. Technol. 2020, 54, 5980−5991

such strong correlations are limited to regions with significant anthropogenic pollution such as the Southeastern United States and China.[10,11,72]

Here, we show that markers of both IEPOX-SOA and MACR-SOA correlate with ambient sulfate but over a range of concentrations covering much cleaner conditions than previously reported.[10,11,51,72] Molecular tracers are well correlated even at concentrations of particulate sulfate <0.5 $\mu g\ m^{-3}$ (Figure 1) representing Amazon basin background conditions and at times preindustrial conditions.[13,73−75] In these environments, IEPOX-SOA tracers (2-MTs + C5ALKTRIOLS) (Figure 1a) contribute significantly more mass to SOA than the MACR-SOA tracer (2-MG) (Figure 1b). IEPOX-SOA tracers correlate moderately with sulfate across all three campaigns (Table S3: $R^2$ = 0.48; 0.49; 0.57; 0.40 for SOAS; wet season; dry season; all data sets, respectively), similar to or higher than previous reports of tracers[10,11] and the IEPOX-SOA statistical factor.[9,13,29,34] 2-MG contributes more mass in SOAS data than GoAmazon but is only weakly correlated with sulfate during all campaigns (Table S3: $R^2$ < 0.25 for each data set). We keep in mind that correlations can also be affected by atmospheric transport including dispersion/dilution and wet deposition. Despite marginal correlation between 2-MG and sulfate and the offset in magnitude between SOAS and GoAmazon, we demonstrate that correlations are improved by accounting for OS formations.

*3.2.2. OS Formations Differ by $HO_2/NO_x$ Pathway and Environment.* OSs formed from chemical reaction of isoprene-derived intermediates and sulfate in the aqueous phase contribute a substantial fraction of isoprene-SOA.[14,41,42,61,76−78] Here, OS analysis included MT-OSs from IEPOX ("OS-216")[5,21,22] and 2-MG-OS ("OS-200"), which can be derived along the MACR-SOA (isoprene/$NO_x$) pathway from 2-MG[5] and HMML/MAE.[47] We explore the relative distribution of the isoprene-derived SOA organic carbon mass in molecular tracers measured by SV-TAG, versus OS forms (offline filter analysis).

Summed particle-phase isoprene-SOA tracers (SV-TAG molecular tracers and OS organic carbon) contribute on average 11, 13, and 14% of the total $PM_1$ organic mass for SOAS, the GoAmazon wet season, and the GoAmazon dry season, respectively. Figure 2 shows the distribution of isoprene-SOA tracers, including OSs, across the three deployments. For the IEPOX-SOA pathway, similar fractions as MT-OSs are present across all campaigns (23−28%), leading to similar trends between data in Figure 1a and Figure 1c (summation of 2-MTs, C5ALKTRIOLS, and MT-OS organic carbon) but with a vertical offset. A similar correlation with sulfate (Table S3; $R^2$ = 0.41 accounting for OSs vs $R^2$ = 0.40 excluding OSs) is observed. Figure 2 shows that the MACR-SOA pathway is only a few percent of the observed isoprene-SOA. However, most MACR-SOA pathway mass during GoAmazon is bound with sulfate as 2-MG-OS, whereas in SOAS, the distribution is almost even between 2-MG and 2-MG-OS. Thus, combining 2-MG-OS organic mass with 2-MG (Figure 1d) increases total accounted MACR-SOA by more than an order of magnitude for GoAmazon data than that accounted in Figure 1b, also revealing sulfate as an important nucleophile in MACR-SOA formation. Accounting for GoAmazon 2-MG-OS carbon, the correlation of MACR-SOA tracers with sulfate (Table S5; $R^2$ = 0.33) is slightly improved (Table S3; $R^2$ < 0.25 each data set), comparable to previous reports ($R^2 \leq 0.33$),[10,11,72] but extended here to levels of

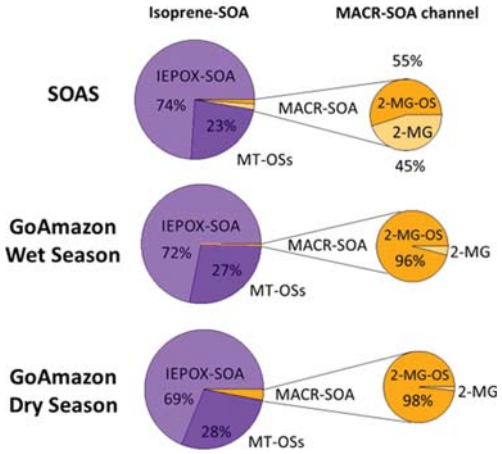


**Figure 2.** Distribution of isoprene-derived SOA mass between IEPOX-SOA (purple) molecular tracers (2-MTs, C5ALKTRIOLS, and MT-OSs) and MACR-SOA (orange) molecular tracers (2-MG and 2-MG-OS) for SOAS (top), the GoAmazon wet season (middle), and the GoAmazon dry season (bottom).

sulfate <1 $\mu g\ m^{-3}$. The correlation is in fact much stronger than previous reports[10,11,72] if data with sulfate ≤1 $\mu g\ m^{-3}$ are considered (Table S5; $R^2$ = 0.66), as there may be a threshold in MACR-SOA at >1 $\mu g\ m^{-3}$ sulfate concentrations. In contrast, there is no apparent threshold for IEPOX-SOA over the sulfate concentrations observed. Since previous observations of the MACR-SOA correlation with sulfate are typically reported for conditions with sulfate concentrations >1 $\mu g\ m^{-3}$, this could be why the role of sulfate in the MACR-SOA pathway has been less clear by $R^2$. Further, although sulfate and 2-MG levels are higher during SOAS than during GoAmazon (Figure S1 and Figure 1), the lower 2-MG-OS fraction may result from higher sulfate and free acids in hydrated particles leading to hydrolysis of 2-MG-OS to 2-MG.[48] With increasing acidity, 2-MG partitions to the gas phase (see Section 3.3.1), which may weaken the correlation with higher sulfate levels. Additional differences might include the relative yields of HMML/MAE formed from MACR[79] as 2-MG precursors, phase state, morphology, or viscosity.

Linear regressions of data across all three deployments reflect different relationships between the IEPOX-SOA and MACR-SOA pathways with sulfate (Figure 1). Data in Figure 1c,d were binned (five data points each), and a linear fit was performed on the means of all bins (Figure S2 and Tables S4 and S5). Tracers of both formation pathways correlate with sulfate (IEPOX-SOA: slope = 490.73 ± 35, $R^2$ = 0.88; MACR-SOA: slope = 5.70 ± 1.28, $R^2$ = 0.59). Units of slopes are ng $m^{-3}$ IEPOX or MACR-SOA tracers, respectively, per $\mu g\ m^{-3}$ particulate sulfate. GoAmazon data are situated within fairly distinct ranges of sulfate with little overlap (Figure 1). SOAS data, while typically within sulfate >1 $\mu g\ m^{-3}$, does show a similar trend down to lower sulfate levels overlapping GoAmazon data for the case of IEPOX-SOA, but there is very little overlap in measurements from different deployments <1 $\mu g\ m^{-3}$ sulfate for MACR-SOA.

From an air quality perspective, assuming that sulfate is a primary driver of isoprene-SOA formation,[5,9,10,34,58,69,80] these quantitative relationships suggest that every 1 $\mu g\ m^{-3}$ reduction in sulfate can lead to at least ~0.5 $\mu g\ m^{-3}$ reduction of these tracers contributing to isoprene-SOA, at least over sulfate and $NO_y$ ranges observed here. Previous studies for the



https://dx.doi.org/10.1021/acs.est.0c00805
Environ. Sci. Technol. 2020, 54, 5980−5991

Southeastern United States also suggested that reductions in $SO_2$ (taken as reductions in sulfate) lead to significant decreases in SOA[81] from isoprene.[9,12,26,29,69] This idea is extended here to the measurements taken during the GoAmazon wet season characterized by relatively low levels of sulfate, which can represent preindustrial conditions, suggesting that natural sources of $SO_2$ also control SOA yield from isoprene oxidation. For the Amazon basin, low "background" sulfate levels can be attributed to biogenic sources such as DMSO and $H_2S$ as well as long-range transport of (anthropogenic) sulfate sources.[13,73,75,82,83] Higher sulfate levels were observed during the GoAmazon dry season, some attributable to biomass burning[84] and not due to seasonal changes in anthropogenic activity at Manaus. We surmise that sulfate concentrations are higher relative to the wet season in part because there is less wet deposition due to precipitation and lower ventilation rates in the dry season. In contrast, higher concentrations of sulfate (some similar to levels observed during the dry season of central Amazon) observed in the Southeastern United States are reasonably attributable to anthropogenic activity.[68,85]

Overall, these results further corroborate aerosol sulfate as a strong determinant of isoprene-SOA formation over a wide range of environments. Importantly though, we find that this correlation holds across three orders of magnitude down to low levels likely representative of preindustrial conditions and is also revealed here to be true for the isoprene/$NO_x$ channel. While 2-MG-OS at SOAS is a reflection of anthropogenic influence from $NO_x$ and $SO_2$ emissions, natural $NO_x$ emissions in the Amazon are sufficient to sustain isoprene/$NO_x$ pathways to form MACR-SOA during the wet season.[63] This suggests that even background/natural isoprene-derived SOA is enhanced by natural sulfate and that sulfate is likely the limiting reagent given plenty of gas-phase production of IEPOX and HMML/MAE for the isoprene/$HO_2$ and isoprene $NO_x$ channels, respectively. As Riva et al.[14] suggested for pristine central Amazon conditions, over 80% of the inorganic sulfate converts to organosulfur via reaction with IEPOX. Further, GoAmazon particles can be more acidic compared to areas with greater anthropogenic $NH_{3(g)}$ emissions, promoting relatively greater OS formation from isoprene.[61] Thus, we infer that under natural conditions in regions with high isoprene emissions, preindustrial aerosol sulfate was likely almost exclusively OSs derived from isoprene. Because OS and inorganic sulfate differ in water uptake properties,[86,87] this implies that preindustrial aerosol sulfate (albeit less abundant) may have been less reflective than current models assume.

**3.3. Role of Particle Acidity.** While sulfate is known to affect and correlate with particle pH (Figure S3), the separate influence of particle acidity on isoprene-SOA formation remains unclear. Laboratory studies demonstrated particle acidity enhances IEPOX uptake[24,27] and MACR-SOA.[48,88] Higher dry season IEPOX-SOA tracer concentrations compared to those in wet and transition seasons of 2002 in another region of the Amazon Basin were attributed in part to increased aerosol acidity by contrasting concentrations of acidic gases, sulfate, and nitrate anions.[36] Online measurements of $PM_1$ composition conducted here now allow for explicit correlations of these tracers with pH, although they are not found to be significantly correlated (Table S3) nor are there appreciable differences in particle acidity between the seasons observed (Figure S3). This further supports that sulfate is a primary driver of the observed tracer concentrations as discussed before. Other field measurements of isoprene-SOA molecular markers show no significant correlations with calculated pH,[10,11,51,89] often ascribed to measurements within a small pH range and possible conflating effects of regional transport where calculated pH for conditions at a field site are not necessarily representative of aerosol acidity at the time/place where pH-dependent chemistry occurs. We also do not observe significant correlations between concentrations of individual IEPOX-SOA and MACR-SOA markers and pH (Table S3), except for a slight to moderate correlation when considering gas + particle 2-MG ($R^2$ = 0.45; 0.37 for wet season; dry season). This revealed that for the isoprene/$NO_x$ pathway, the distribution of 2-MG between gas and particle phases correlates with pH. For the isoprene/$HO_2$ pathway, we later reveal correlation between pH and the ratio of IEPOX-SOA markers, 2-MTs and C5ALKTRIOLS.

*3.3.1. Particle Acidity and Liquid Water Content Affecting MACR-SOA Phase Distribution.* Figure 3 shows that the 2-MG mass fraction in the particle phase, $F_p$, correlates with pH during GoAmazon dry season ($R^2$ = 0.55). The particle-phase concentration is in fact relatively constant over a range of pH values (0−3) for all three data sets (Figure S4). However, when considering gas-phase concentration, calculated as the difference between SV-TAG total (gas + particle) and particle channels, there is a decrease with increasing pH most obvious during GoAmazon (Figure S5). That is, 2-MG increasingly partitions to the gas phase with increasing acidity. No/weak correlations of 2-MG with acidity have otherwise been observed from other field studies in the United States,[8,10,11,51] possibly due to methods of utilizing filter-based measurements which can suffer from artifacts of gas-phase adsorption, averaging due to lower time resolution, and field observations that typically fall within narrow pH ranges (often below pH = 2). SOAS data lie in a narrow range of calculated pH (0.25−1.0) and exhibit wider variation though higher average $F_p$ values for the same pH range as in GoAmazon (Figure 3). The variation may be due to other factors of liquid water content, ion activity, organics, and phase that affect 2-MG accommodation for SOAS conditions. More highly viscous and

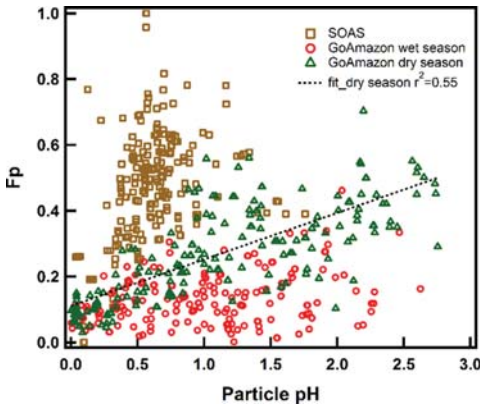


**Figure 3.** Fraction of 2-MG in the particle phase and associated particle pH during SOAS (brown squares), the GoAmazon wet season (red circles), and the GoAmazon dry season (green triangles). Data smoothed using a running-median smoothing algorithm. Best fit line (dashed) for the GoAmazon dry season shown with slope = 0.14 and $R^2$ = 0.55. Best fit lines for other campaigns not shown due to poor correlations ($R^2$ < 0.2).



https://dx.doi.org/10.1021/acs.est.0c00805
Environ. Sci. Technol. 2020, 54, 5980−5991

coated organic particles could lead to less 2-MG repartitioning back to the gas phase, keeping $F_p$ values higher than expected from 2-MG vapor pressure.[43] In contrast, GoAmazon conditions comprise wider ranges in particle acidity and LWC associated with changes in 2-MG concentrations and observed $F_p$. The strongest trend for SOAS 2-MG is with LWC (Figure S6) revealed in the total (gas + particle) channel; total 2-MG decreases with increasing LWC, again mostly associated with a decreasing gas-phase concentration as associated decreases in particle phase 2-MG are more modest (Figure S7). These measurements are the first field observation of pH- and LWC-dependent 2-MG accommodation in accordance to laboratory measurements[48] in which gaseous 2-MG concentrations were observed to increase in the headspace over increasingly acidic solutions. This also suggests that for particles that are more acidic, more carbon through the MACR-SOA pathway recycles back to the gas phase after MAE/HMML uptake if no limitations to gas-particle exchange exist. In other words, the extent to which the particle phase acts as a reservoir of $NO_x$-derived organic species is pH-dependent for GoAmazon conditions. This further implies that PM formation along this route may be minimized by decreasing particle pH as Nguyen et al.[48] proposed that hydrated particles with higher free acidity might favor monomeric 2-MG and hydrolyze sulfate and nitrate esters,[79] leading to suppression of SOA growth. Still, many other SOA formation mechanisms are more efficient under acidic conditions.[90] Others demonstrated that while $SO_2$ controls have led to lower particulate sulfate in the Southeast United States, PM has remained acidic.[68,91] While GoAmazon data includes pre-anthropogenic sulfate levels much lower than those of SOAS and can be more acidic (associated with higher gas-phase fraction of 2-MG), they are still sufficiently acidic to promote IEPOX and MAE/HMML uptake as well as 2-MG-OS formation. This suggests that isoprene-SOA formation from these pathways is sustained even under natural/background levels of sulfate and $NO_x$, and control of anthropogenic $SO_2$ emissions (as a source of sulfate) remains most effective in limiting SOA formation from both pathways.

*3.3.2. Tracer Ratio Correlations Further Revealing the Role of Acidity.* To better understand chemical controls on distribution of isoprene-derived carbon between different pathways to isoprene-SOA formation, we examine ratios of the SV-TAG-measured molecular tracers as correlated with other chemical parameters. In this section, we do not include carbon associated with OSs because of coarser time resolution of these measurements that would limit the robustness of correlations; we note that scaling tracer concentrations by an average OS contribution would not impact correlations. We first investigate the isoprene/$HO_2$ pathway (i.e., summed 2-MTs and C5ALKTRIOLS) versus the isoprene/$NO_x$ pathway (i.e., 2-MG) as IEPOX-SOA markers/MACR-SOA markers. We further explore branching of IEPOX-SOA carbon between 2-MTs and C5ALKTRIOLS.

*3.3.3. Isoprene/$HO_2$ versus Isoprene/$NO_x$ Pathway Tracer Correlations.* Based on current understandings of isoprene + OH oxidation, it would be expected that the split between carbon associated with the IEPOX-SOA and MACR-SOA pathways would be $NO_y$-dependent. We evaluate the ratio of IEPOX-SOA/MACR-SOA tracers, i.e., (2-MTs + C5ALKTRIOLS)/(2-MG), as correlated with $NO_y$. Using $NO_y$ as a surrogate for integrated exposure of sampled air masses to $NO_x$,[13,63,67] we explore the IEPOX-SOA/MACR-SOA tracers ratio as a proxy for the branching ratio between the isoprene/$HO_2$ versus isoprene/$NO_x$ pathways. While this ratio might be expected to decrease with increasing amount of $NO_y$, correlations were poor regardless of the phase (Table S3). Figure S8 (particle phase) and Figure S9 (total) also show that IEPOX-SOA/MACR-SOA ratios versus $NO_y$ filtered during daytime are still poorly correlated and widely variable across deployments. Very weak although higher $R^2$ values (~0.2 for GoAmazon) are found for IEPOX-SOA/MACR-SOA ratios versus $O_3$ (Table S3), consistent with total 2-MG correlating better with $O_3$ ($R^2$ > 0.3 and up to 0.66) than with $NO_y$ (no correlation). Correlation of 2-MG with $O_3$ (Figures S10 and Figure S11) suggests that $O_3$ is a better indicator of the air mass age than $NO_y$, which is further discussed in the Supporting Information.

*3.3.4. Isoprene/$HO_2$ Tracers Ratio Is pH-Dependent.* Limited studies have probed chemical controls on relative yields of IEPOX-SOA tracers, 2-MTs and C5ALKTRIOLS.[21,23,71] Formation of C5ALKTRIOLS has been explained by acid-catalyzed ring opening of isoprene epoxydiols.[38] Recent work suggests some fraction derives from decomposition of OSs and their oligomers thereof in some analytical techniques,[42] which may be representative of a tendency for many of these tracers to be formed by (thermal) decomposition during analysis.[44,45,92] Testing of MT-OSs in SV-TAG (see the Supporting Information) suggests they would be a minor contribution (<10% by mass) to 2-MTs and C5ALKTRIOLS observed here. The extent to which a given compound represents a sampled atmospheric constituent versus a transformed product of analysis remains an active area of methodological research. Here, we use these tracers as useful known indicators of isoprene oxidation, and we evaluate the extent to which different compound classes represent different formation pathways and can provide insight into particle-formation chemistry.

Plots of 2-MTs versus C5ALKTRIOLS reveal that the distribution of IEPOX-derived carbon (as inferred from the slope of the best fit line) and correlation between these analytes varies across these deployments Figure 4. 2-MTs/C5ALKTRIOLS is 0.52 with $R^2$ = 0.16 for SOAS (Figure 4a), 0.27 with $R^2$ = 0.54 for the GoAmazon wet season (Figure 4b), and 0.17 with $R^2$ = 0.72 for the GoAmazon dry season (Figure 4c). The variability in ratio and correlation of these tracers indicate that these analytes derive from distinct chemical conditions and possibly from additional precursors besides IEPOX. For example, 2-MTs were observed in SOA generated from isoprene ozonolysis under laboratory conditions,[60,93] although correlations of 2-MTs with $O_3$ are too poor in these data sets to suggest it as a leading source (Table S3).

The strongest explanatory variable for 2-MTs/C5ALKTRIOLS is pH ($R^2$ = 0.14 for GoAmazon wet season, $R^2$ = 0.42 for GoAmazon dry season, Table S3 and Figure 4d). No trend with regard to pH is observed for SOAS and most data fall within pH = 0.5 ± 0.5. This correlation was the most obvious in GoAmazon data sets (Figure 4), where particle pH ranges more widely (0−3). As pH decreases, 2-MTs/C5ALKTRIOLS also decreases, suggesting that C5ALKTRIOLS formation is enhanced with increasing particle acidity (Figure 4d).[38] It is important to note that pH is a modeled output, and we keep in mind that the calculated pH values here result from assuming instantaneous gas-particle equilibrium. This assumption seems valid for liquid-phase organic aerosols observed in GoAmazon[94] and SOAS.[95] While



https://dx.doi.org/10.1021/acs.est.0c00805
Environ. Sci. Technol. 2020, 54, 5980−5991

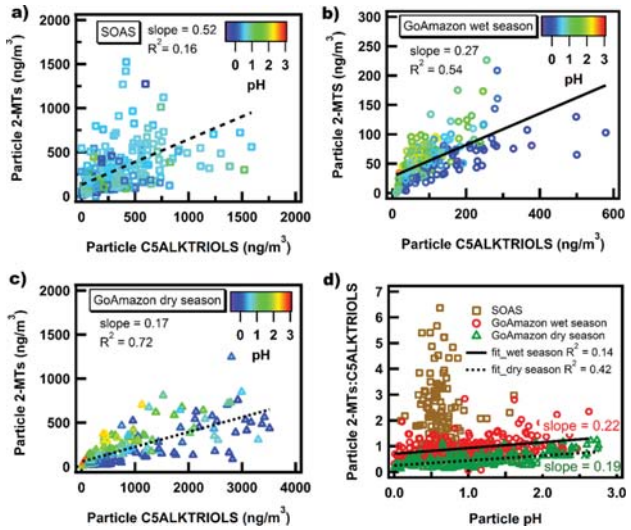


**Figure 4.** Particle phase 2-MTs vs C5ALKTRIOLS during (a) SOAS, (b) the GoAmazon wet season, and (c) the GoAmazon dry season. Best fit lines for each data set shown along with the slope and $R^2$ values. Data are colored by particle pH, revealing some correlation of 2-MTs/C5ALKTRIOLS with pH for GoAmazon data sets. (d) Ratio of particle-phase 2-MTs and C5ALKTRIOLS vs particle pH for SOAS (brown squares), the GoAmazon wet season (red circles), and the GoAmazon dry season (green triangles). Best fit lines for the GoAmazon wet season (solid line, slope = 0.22, $R^2$ = 0.14) and the GoAmazon dry season (dotted line, slope = 0.19, $R^2$ = 0.42).

RH and hence LWC can be highly variable as particles move about in daytime turbulence within the boundary layer, modeled pH may not reflect pH when IEPOX-SOA markers actually form, as limitations of the calculation have been discussed.[13,43] Still, we find that it is a useful metric for assessing particle-phase chemical conditions at the time these markers are measured. That is, concerted effects of RH, $T$, and gas/particle composition (e.g., sulfate, LWC, organics) are captured in calculated pH, and the 2-MTS/C5ALKTRIOLS ratio serves as a useful indicator of IEPOX-SOA formation under varying chemical conditions.

## 4. ATMOSPHERIC IMPLICATIONS

We provide the first ambient measurements revealing strong correlations with pH impacting tracer ratios derived in the isoprene/$HO_2$ pathway (allowing for mechanistic insight) and phase partitioning of the isoprene/$NO_x$ pathway tracer, 2-methylglyceric acid. Further, while the role of sulfate in isoprene-SOA formation has been studied, it has primarily been interpreted as a role of anthropogenically-derived sulfate enhancing SOA formation. We show here by contrasting SOAS and GoAmazon that naturally derived sulfate also enhances isoprene-SOA formation. In particular, the relatively greater incorporation of naturally derived sulfate into organosulfates under the isoprene/$NO_x$ channel during GoAmazon highlights the impact of more highly acidic particle conditions found in an environment representative of preindustrial conditions, as well as the fact that sulfate may be a stronger nucleophile than previously revealed for this pathway. Organosulfates are typically interpreted as markers of anthropogenic influence on SOA formation, which we demonstrate is not always the case, with implications for how such compounds are represented in global models of SOA and for the chemical composition and properties of preindustrial SOA.

## ■ ASSOCIATED CONTENT

### Supporting Information

The Supporting Information is available free of charge at https://pubs.acs.org/doi/10.1021/acs.est.0c00805.

Additional details of Materials and Methods, 2-MG correlation with ozone, figures of campaign comparisons, select tracer correlations, and a complete table of coefficients of determination for all calculated tracer correlations. (PDF)

## ■ AUTHOR INFORMATION


### Corresponding Authors

**Lindsay D. Yee** − *Department of Environmental Science, Policy, and Management, University of California, Berkeley, California 94720, United States;* orcid.org/0000-0001-8965-9319; Email: lindsay.yee@berkeley.edu

**Allen H. Goldstein** − *Department of Environmental Science, Policy, and Management and Department of Civil and Environmental Engineering, University of California, Berkeley, California 94720, United States;* Email: ahg@berkeley.edu

### Authors

**Gabriel Isaacman-VanWertz** − *Department of Environmental Science, Policy, and Management, University of California, Berkeley, California 94720, United States;* orcid.org/0000-0002-3717-4798

**Rebecca A. Wernis** − *Department of Civil and Environmental Engineering, University of California, Berkeley, California 94720, United States*

**Nathan M. Kreisberg** − *Aerosol Dynamics Inc., Berkeley, California 94710, United States*

**Marianne Glasius** − *Department of Chemistry, Aarhus University, 8000 Aarhus C, Denmark;* orcid.org/0000-0002-4404-6989

**Matthieu Riva** − *Department of Environmental Sciences and Engineering, Gillings School of Global Public Health, University of North Carolina, Chapel Hill, North Carolina 27599, United States;* orcid.org/0000-0003-0054-4131

**Jason D. Surratt** − *Department of Environmental Sciences and Engineering, Gillings School of Global Public Health, University of North Carolina, Chapel Hill, North Carolina 27599, United States;* orcid.org/0000-0002-6833-1450

**Suzane S. de Sá** − *School of Engineering and Applied Sciences, Harvard University, Cambridge, Massachusetts 01451, United States*

**Scot T. Martin** − *School of Engineering and Applied Sciences and Department of Earth and Planetary Sciences, Harvard University, Cambridge, Massachusetts 01451, United States;* orcid.org/0000-0002-8996-7554

**M. Lizabeth Alexander** − *Environmental Molecular Sciences Laboratory, Pacific Northwest National Laboratory, Richland, Washington 99352, United States*

**Brett. B. Palm** − *Department of Chemistry & Biochemistry and Cooperative Institute for Research in Environmental Sciences (CIRES), University of Colorado, Boulder, Colorado 80309, United States*

**Weiwei Hu** − *Department of Chemistry & Biochemistry and Cooperative Institute for Research in Environmental Sciences*




https://dx.doi.org/10.1021/acs.est.0c00805
Environ. Sci. Technol. 2020, 54, 5980−5991

(CIRES), University of Colorado, Boulder, Colorado 80309, United States

**Pedro Campuzano-Jost** − *Department of Chemistry & Biochemistry and Cooperative Institute for Research in Environmental Sciences (CIRES), University of Colorado, Boulder, Colorado 80309, United States;* orcid.org/0000-0003-3930-010X

**Douglas A. Day** − *Department of Chemistry & Biochemistry and Cooperative Institute for Research in Environmental Sciences (CIRES), University of Colorado, Boulder, Colorado 80309, United States;* orcid.org/0000-0003-3213-4233

**Jose L. Jimenez** − *Department of Chemistry & Biochemistry and Cooperative Institute for Research in Environmental Sciences (CIRES), University of Colorado, Boulder, Colorado 80309, United States;* orcid.org/0000-0001-6203-1847

**Yingjun Liu** − *School of Engineering and Applied Sciences, Harvard University, Cambridge, Massachusetts 01451, United States;* orcid.org/0000-0001-6659-3660

**Pawel K. Misztal** − *Department of Environmental Science, Policy, and Management, University of California, Berkeley, California 94720, United States;* orcid.org/0000-0003-1060-1750

**Paulo Artaxo** − *Universidade de São Paulo, São Paulo, Brazil 05508-020*

**Juarez Viegas** − *Instituto Nacional de Pesquisas da Amazonia, Manaus, Amazonas, Brazil 69060-001*

**Antonio Manzi** − *Instituto Nacional de Pesquisas da Amazonia, Manaus, Amazonas, Brazil 69060-001*

**Rodrigo A. F. de Souza** − *Universidade do Estado do Amazonas, Manaus, Amazonas, Brazil 69735-000*

**Eric S. Edgerton** − *Atmospheric Research & Analysis, Inc., Cary, North Carolina 27513, United States*

**Karsten Baumann** − *Atmospheric Research & Analysis, Inc., Cary, North Carolina 27513, United States*

Complete contact information is available at: https://pubs.acs.org/10.1021/acs.est.0c00805

### Notes

The authors declare no competing financial interest.

## ■ ACKNOWLEDGMENTS

L.D.Y. was supported by the UC Berkeley Chancellor's Postdoctoral Fellowship. G.I.-VW. was supported by the NSF Graduate Research Fellowship (#DGE 1106400). SV-TAG data was collected by G.I.-VW, L.D.Y, N.M.K., and R.A.W. as part of the SOAS and GoAmazon 2014/5 field campaign, funded by NSF Atmospheric Chemistry Program #1250569 and 1332998, respectively. The instrument as deployed was developed through support from the U.S. Department of Energy (DOE) SBIR grant DE-SC0004698 in collaboration with S.V.H. and A.H.G. Data collection and analysis was supported in large part by NSF AGS-1243354 and the DOE Office of Science Office of Biological and Environmental Research (BER), specifically DE-SC0011105 and two user facilities: the Atmospheric Radiation Measurement (ARM) Climate Research Facility and the Environmental Molecular Sciences Laboratory located at Pacific Northwest National Laboratory. This publication was developed under STAR Fellowship Assistance Agreement no. FP-91778401-0 (R.A.W.) and FP-91761701-0 (B.B.P.) and awarded by the U.S. Environmental Protection Agency (EPA). It has not been formally reviewed by the EPA. The views expressed in this publication are solely those of the authors, and the EPA does not endorse any products or commercial services mentioned in this publication. Filter analysis by M.R. and J.D.S was supported by the U.S. EPA (#835404), NOAA Climate Program Office's AC4 Program (#NA13OAR4310064), and the Camille and Henry Dreyfus Postdoctoral Fellowship Program in Environmental Chemistry. We acknowledge the support from the Central Office of the Large Scale Biosphere Atmosphere Experiment in Amazonia (LBA), the Instituto Nacional de Pesquisas da Amazonia (INPA), and the Universidade do Estado do Amazonia (UEA). P.A. acknowledges support from FAPESP through 2013/ 05014-0. The work was conducted under 001030/2012-4 of the Brazilian National Council for Scientific and Technological Development (CNPq). The CU-Boulder group was supported by DOE (BER/ASR) DE-SC0016559 and NSF AGS-1822664.

## ■ REFERENCES

(1) Henze, D. K.; Seinfeld, J. H. Global Secondary Organic Aerosol from Isoprene Oxidation. *Geophys. Res. Lett.* **2006**, *33*, L09812.

(2) Edney, E. O.; Kleindienst, T. E.; Jaoui, M.; Lewandowski, M.; Offenberg, J. H.; Wang, W.; Claeys, M. Formation of 2-Methyl Tetrols and 2-Methylglyceric Acid in Secondary Organic Aerosol from Laboratory Irradiated Isoprene / $NO_X$ / $SO_2$ / Air Mixtures and Their Detection in Ambient PM 2.5 Samples Collected in the Eastern United States. *Atmos. Environ.* **2005**, *39*, 5281−5289.

(3) Kroll, J. H.; Ng, N. L.; Murphy, S. M.; Flagan, R. C.; Seinfeld, J. H. Secondary Organic Aerosol Formation from Isoprene Photooxidation. *Environ. Sci. Technol.* **2006**, *40*, 1869−1877.

(4) Kleindienst, T. E.; Edney, E. O.; Lewandowski, M.; Offenberg, J. H.; Jaoui, M. Secondary Organic Carbon and Aerosol Yields from the Irradiations of Isoprene and α-Pinene in the Presence of $NO_x$ and $SO_2$. *Environ. Sci. Technol.* **2006**, *40*, 3807−3812.

(5) Surratt, J. D.; Kroll, J. H.; Kleindienst, T. E.; Edney, E. O.; Claeys, M.; Sorooshian, A.; Ng, N. L.; Offenberg, J. H.; Lewandowski, M.; Jaoui, M.; Flagan, R. C.; Seinfeld, J. H. Evidence for Organosulfates in Secondary Organic Aerosol. *Environ. Sci. Technol.* **2007**, *41*, 517−527.

(6) Goldstein, A. H.; Koven, C. D.; Heald, C. L.; Fung, I. Y. Biogenic Carbon and Anthropogenic Pollutants Combine to Form a Cooling Haze over the Southeastern United States. *Proc. Natl. Acad. Sci. U. S. A.* **2009**, *106*, 8835−8840.

(7) Shrivastava, M.; Andreae, M. O.; Artaxo, P.; Barbosa, H. M. J.; Berg, L. K.; Brito, J.; Ching, J.; Easter, R. C.; Fan, J.; Fast, J. D.; Feng, Z.; Fuentes, J. D.; Glasius, M.; Goldstein, A. H.; Alves, E. G.; Gomes, H.; Gu, D.; Guenther, A.; Jathar, S. H.; Kim, S.; Liu, Y.; Lou, S.; Martin, S. T.; McNeill, V. F.; Medeiros, A.; de Sá, S. S.; Shilling, J. E.; Springston, S. R.; Souza, R. A. F.; Thornton, J. A.; Isaacman-VanWertz, G.; Yee, L. D.; Ynoue, R.; Zaveri, R. A.; Zelenyuk, A.; Zhao, C. Urban Pollution Greatly Enhances Formation of Natural Aerosols over the Amazon Rainforest. *Nat. Commun* **2019**, *10*, 1046.

(8) Lin, Y.-H.; Knipping, E. M.; Edgerton, E. S.; Shaw, S. L.; Surratt, J. D. Investigating the Influences of $SO_2$ and $NH_3$ Levels on Isoprene-Derived Secondary Organic Aerosol Formation Using Conditional Sampling Approaches. *Atmos. Chem. Phys.* **2013**, *13*, 8457−8470.

(9) Xu, L.; Guo, H.; Boyd, C. M.; Klein, M.; Bougiatioti, A.; Cerully, K. M.; Hite, J. R.; Isaacman-VanWertz, G.; Kreisberg, N. M.; Knote, C.; Olson, K.; Koss, A.; Goldstein, A. H.; Hering, S. V.; de Gouw, J.; Baumann, K.; Lee, S.-H.; Nenes, A.; Weber, R. J.; Ng, N. L. Effects of Anthropogenic Emissions on Aerosol Formation from Isoprene and Monoterpenes in the Southeastern United States. *Proc. Natl. Acad. Sci.* **2015**, *112*, 37−42.

(10) Budisulistiorini, S. H.; Li, X.; Bairai, S. T.; Renfro, J.; Liu, Y.; Liu, Y. J.; Mckinney, K. A.; Martin, S. T.; Mcneill, V. F.; Pye, H. O. T.; Nenes, A.; Neff, M. E.; Stone, E. A.; Mueller, S.; Knote, C.; Shaw, S. L.; Zhang, Z.; Gold, A.; Surratt, J. D. Examining the Effects of Anthropogenic Emissions on Isoprene-Derived Secondary Organic

Aerosol Formation during the 2013 Southern Oxidant and Aerosol Study (SOAS) at the Look Rock, Tennessee Ground Site. *Atmos. Chem. Phys.* **2015**, *15*, 8871−8888.
(11) Rattanavaraha, W.; Chu, K.; Budisulistiorini, S. H.; Riva, M.; Lin, Y.-H.; Edgerton, E. S.; Baumann, K.; Shaw, S. L.; Guo, H.; King, L.; Weber, R. J.; Neff, M. E.; Stone, E. A.; Offenberg, J. H.; Zhang, Z.; Gold, A.; Surratt, J. D. Assessing the Impact of Anthropogenic Pollution on Isoprene-Derived Secondary Organic Aerosol Formation in PM 2.5 Collected from the Birmingham, Alabama, Ground Site during the 2013 Southern Oxidant and Aerosol Study. *Atmos. Chem. Phys.* **2016**, *16*, 4897−4914.
(12) Budisulistiorini, S. H.; Nenes, A.; Carlton, A. G.; Surratt, J. D.; McNeill, V. F.; Pye, H. O. T. Simulating Aqueous-Phase Isoprene-Epoxydiol (IEPOX) Secondary Organic Aerosol Production During the 2013 Southern Oxidant and Aerosol Study (SOAS). *Environ. Sci. Technol.* **2017**, *51*, 5026−5034.
(13) de Sá, S. S.; Palm, B. B.; Campuzano-Jost, P.; Day, D. A.; Newburn, M. K.; Hu, W.; Isaacman-VanWertz, G.; Yee, L. D.; Thalman, R.; Brito, J.; Carbone, S.; Artaxo, P.; Goldstein, A. H.; Manzi, A. O.; Souza, R. A. F.; Mei, F.; Shilling, J. E.; Springston, S. R.; Wang, J.; Surratt, J. D.; Lizabeth Alexander, M.; Jimenez, J. L.; Martin, S. T. Influence of Urban Pollution on the Production of Organic Particulate Matter from Isoprene Epoxydiols in Central Amazonia. *Atmos. Chem. Phys.* **2017**, *17*, 6611−6629.
(14) Riva, M.; Chen, Y.; Zhang, Y.; Lei, Z.; Olson, N. E.; Boyer, H. C.; Narayan, S.; Yee, L. D.; Green, H. S.; Cui, T.; Zhang, Z.; Baumann, K.; Fort, M.; Edgerton, E.; Budisulistiorini, S. H.; Rose, C. A.; Ribeiro, I. O.; e Oliveira, R. L.; dos Santos, E. O.; Machado, C.; Szopa, S.; Zhao, Y.; Alves, E. G.; de Sá, S. S.; Hu, W.; Knipping, E. M.; Shaw, S. L.; Duvoisin Junior, S.; de Souza, R. A. F.; Palm, B. B.; Jimenez, J.-L.; Glasius, M.; Goldstein, A. H.; Pye, H. O. T.; Gold, A.; Turpin, B. J.; Vizuete, W.; Martin, S. T.; Thornton, J. A.; Dutcher, C. S.; Ault, A. P.; Surratt, J. D. Increasing Isoprene Epoxydiol-to-Inorganic Sulfate Aerosol Ratio Results in Extensive Conversion of Inorganic Sulfate to Organosulfur Forms: Implications for Aerosol Physicochemical Properties. *Environ. Sci. Technol.* **2019**, *53*, 8682−8694.
(15) Surratt, J. D.; Murphy, S. M.; Kroll, J. H.; Ng, N. L.; Hildebrandt, L.; Sorooshian, A.; Szmigielski, R.; Vermeylen, R.; Maenhaut, W.; Claeys, M.; Flagan, R. C.; Seinfeld, J. H. Chemical Composition of Secondary Organic Aerosol Formed from the Photooxidation of Isoprene. *J. Phys. Chem. A* **2006**, *110*, 9665−9690.
(16) Wang, W.; Iinuma, Y.; Kahnt, A.; Ryabtsova, O.; Mutzel, A.; Vermeylen, R.; Van der Veken, P.; Maenhaut, W.; Herrmann, H.; Claeys, M. Formation of Secondary Organic Aerosol Marker Compounds from the Photooxidation of Isoprene and Isoprene-Derived Alkene Diols under Low-NOx Conditions. *Faraday Discuss.* **2013**, *165*, 261.
(17) Chan, A. W. H.; Chan, M. N.; Surratt, J. D.; Chhabra, P. S.; Loza, C. L.; Crounse, J. D.; Yee, L. D.; Flagan, R. C.; Wennberg, P. O.; Seinfeld, J. H. Role of Aldehyde Chemistry and $NO_x$ Concentrations in Secondary Organic Aerosol Formation. *Atmos. Chem. Phys.* **2010**, *10*, 7169−7188.
(18) Xu, L.; Kollman, M. S.; Song, C.; Shilling, J. E.; Ng, N. L. Effects of NOx on the Volatility of Secondary Organic Aerosol from Isoprene Photooxidation. *Environ. Sci. Technol.* **2014**, *48*, 2253−2262.
(19) Liu, J.; D'Ambro, E. L.; Lee, B. H.; Lopez-Hilfiker, F. D.; Zaveri, R. A.; Rivera-Rios, J. C.; Keutsch, F. N.; Iyer, S.; Kurten, T.; Zhang, Z.; Gold, A.; Surratt, J. D.; Shilling, J. E.; Thornton, J. A. Efficient Isoprene Secondary Organic Aerosol Formation from a Non-IEPOX Pathway. *Environ. Sci. Technol.* **2016**, *50*, 9872−9880.
(20) Wennberg, P. O.; Bates, K. H.; Crounse, J. D.; Dodson, L. G.; McVay, R. C.; Mertens, L. A.; Nguyen, T. B.; Praske, E.; Schwantes, R. H.; Smarte, M. D.; St Clair, J. M.; Teng, A. P.; Zhang, X.; Seinfeld, J. H. Gas-Phase Reactions of Isoprene and Its Major Oxidation Products. *Chem. Rev.* **2018**, *118*, 3337−3390.
(21) Surratt, J. D.; Chan, A. W. H.; Eddingsaas, N. C.; Chan, M.; Loza, C. L.; Kwan, A. J.; Hersey, S. P.; Flagan, R. C.; Wennberg, P. O.; Seinfeld, J. H. Reactive Intermediates Revealed in Secondary Organic Aerosol Formation from Isoprene. *Proc. Natl. Acad. Sci. U. S. A.* **2010**, *107*, 6640−6645.
(22) Lin, Y.-H.; Zhang, Z.; Docherty, K. S.; Zhang, H.; Budisulistiorini, S. H.; Rubitschun, C. L.; Shaw, S. L.; Knipping, E. M.; Edgerton, E. S.; Kleindienst, T. E.; Gold, A.; Surratt, J. D. Isoprene Epoxydiols as Precursors to Secondary Organic Aerosol Formation: Acid-Catalyzed Reactive Uptake Studies with Authentic Compounds. *Environ. Sci. Technol.* **2012**, *46*, 250−258.
(23) Riedel, T. P.; Lin, Y.-H.; Zhang, Z.; Chu, K.; Thornton, J. A.; Vizuete, W.; Gold, A.; Surratt, J. D. Constraining Condensed-Phase Formation Kinetics of Secondary Organic Aerosol Components from Isoprene Epoxydiols. *Atmos. Chem. Phys.* **2016**, *16*, 1245−1254.
(24) Surratt, J. D.; Lewandowski, M.; Offenberg, J. H.; Jaoui, M.; Kleindienst, T. E.; Edney, E. O.; Seinfeld, J. H. Effect of Acidity on Secondary Organic Aerosol Formation from Isoprene. *Environ. Sci. Technol.* **2007**, *41*, 5363−5369.
(25) Woo, J. L.; McNeill, V. F. SimpleGAMMA v1.0 − a Reduced Model of Secondary Organic Aerosol Formation in the Aqueous Aerosol Phase (AaSOA). *Geosci. Model Dev.* **2015**, *8*, 1821−1829.
(26) Pye, H. O. T.; Pinder, R. W.; Piletic, I. R.; Xie, Y.; Capps, S. L.; Lin, Y.-H.; Surratt, J. D.; Zhang, Z.; Gold, A.; Luecken, D. J.; Hutzell, W. T.; Jaoui, M.; Offenberg, J. H.; Kleindienst, T. E.; Lewandowski, M.; Edney, E. O. Epoxide Pathways Improve Model Predictions of Isoprene Markers and Reveal Key Role of Acidity in Aerosol Formation. *Environ. Sci. Technol.* **2013**, *47*, 11056−11064.
(27) Gaston, C. J.; Riedel, T. P.; Zhang, Z.; Gold, A.; Surratt, J. D.; Thornton, J. A. Reactive Uptake of an Isoprene-Derived Epoxydiol to Submicron Aerosol Particles. *Environ. Sci. Technol.* **2014**, *48*, 11178−11186.
(28) Riedel, T. P.; Lin, Y.-H.; Budisulistiorini, S. H.; Gaston, C. J.; Thornton, J. A.; Zhang, Z.; Vizuete, W.; Gold, A.; Surratt, J. D. Heterogeneous Reactions of Isoprene-Derived Epoxides: Reaction Probabilities and Molar Secondary Organic Aerosol Yield Estimates. *Environ. Sci. Technol. Lett.* **2015**, *2*, 38−42.
(29) Marais, E. A.; Jacob, D. J.; Jimenez, J. L.; Campuzano-Jost, P.; Day, D. A.; Hu, W.; Krechmer, J.; Zhu, L.; Kim, P. S.; Miller, C. C.; Fisher, J. A.; Travis, K.; Yu, K.; Hanisco, T. F.; Wolfe, G. M.; Arkinson, H. L.; Pye, H. O. T.; Froyd, K. D.; Liao, J.; McNeill, V. F. Aqueous-Phase Mechanism for Secondary Organic Aerosol Formation from Isoprene : Application to the Southeast United States and Co-Benefit of $SO_2$ Emission Controls. *Atmos. Chem. Phys.* **2016**, *16*, 1603−1618.
(30) Paulot, F.; Crounse, J. D.; Kjaergaard, H. G.; Kürten, A.; St. Clair, J. M.; Seinfeld, J. H.; Wennberg, P. O. Unexpected Epoxide Formation in the Gas-Phase Photooxidation of Isoprene. *Science* **2009**, *325*, 730−733.
(31) Liu, Y.; Kuwata, M.; Strick, B. F.; Geiger, F. M.; Thomson, R. J.; McKinney, K. A.; Martin, S. T. Uptake of Epoxydiol Isomers Accounts for Half of the Particle-Phase Material Produced from Isoprene Photooxidation via the HO 2 Pathway. *Environ. Sci. Technol.* **2015**, *49*, 250−258.
(32) Bates, K. H.; Crounse, J. D.; St. Clair, J. M.; Bennett, N. B.; Nguyen, T. B.; Seinfeld, J. H.; Stoltz, B. M.; Wennberg, P. O. Gas Phase Production and Loss of Isoprene Epoxydiols. *J. Phys. Chem. A* **2014**, *118*, 1237−1246.
(33) Nguyen, T. B.; Coggon, M. M.; Bates, K. H.; Zhang, X.; Schwantes, R. H.; Schilling, K. A.; Loza, C. L.; Flagan, R. C.; Wennberg, P. O.; Seinfeld, J. H. Organic Aerosol Formation from the Reactive Uptake of Isoprene Epoxydiols (IEPOX) onto Non-Acidified Inorganic Seeds. *Atmos. Chem. Phys.* **2014**, *14*, 3497−3510.
(34) Budisulistiorini, S. H.; Canagaratna, M. R.; Croteau, P. L.; Marth, W. J.; Baumann, K.; Edgerton, E. S.; Shaw, S. L.; Knipping, E. M.; Worsnop, D. R.; Jayne, J. T.; Gold, A.; Surratt, J. D. Real-Time Continuous Characterization of Secondary Organic Aerosol Derived from Isoprene Epoxydiols in Downtown Atlanta, Georgia, Using the Aerodyne Aerosol Chemical Speciation Monitor. *Environ. Sci. Technol.* **2013**, *47*, 5686−5694.
(35) Claeys, M.; Graham, B.; Vas, G.; Wang, W.; Vermeylen, R.; Pashynska, V.; Cafmeyer, J.; Guyon, P.; Andreae, M. O.; Artaxo, P.;


https://dx.doi.org/10.1021/acs.est.0c00805
*Environ. Sci. Technol.* 2020, 54, 5980−5991

Maenhaut, W. Formation of Secondary Organic Aerosols through Photooxidation of Isoprene. *Science* **2004**, *303*, 1173−1176.
(36) Claeys, M.; Kourtchev, I.; Pashynska, V.; Vas, G.; Vermeylen, R.; Wang, W.; Cafmeyer, J.; Chi, X.; Artaxo, P.; Andreae, M. O.; Maenhaut, W. Polar Organic Marker Compounds in Atmospheric Aerosols during the LBA-SMOCC 2002 Biomass Burning Experiment in Rondônia, Brazil: Sources and Source Processes, Time Series, Diel Variations and Size Distributions. *Atmos. Chem. Phys.* **2010**, *10*, 9319−9331.
(37) Lin, Y.-H.; Budisulistiorini, S. H.; Chu, K.; Siejack, R. A.; Zhang, H.; Riva, M.; Zhang, Z.; Gold, A.; Kautzman, K. E.; Surratt, J. D. Light-Absorbing Oligomer Formation in Secondary Organic Aerosol from Reactive Uptake of Isoprene Epoxydiols. *Environ. Sci. Technol.* **2014**, *48*, 12012−12021.
(38) Wang, W.; Kourtchev, I.; Graham, B.; Cafmeyer, J.; Maenhaut, W.; Claeys, M. Characterization of Oxygenated Derivatives of Isoprene Related to 2-Methyltetrols in Amazonian Aerosols Using Trimethylsilylation and Gas Chromatography/Ion Trap Mass Spectrometry. *Rapid Commun. Mass Spectrom.* **2005**, *19*, 1343−1351.
(39) Kleindienst, T. E.; Lewandowski, M.; Offenberg, J. H.; Jaoui, M.; Edney, E. O. The Formation of Secondary Organic Aerosol from the Isoprene + OH Reaction in the Absence of $NO_X$. *Atmos. Chem. Phys.* **2009**, *9*, 6541−6558.
(40) Froyd, K. D.; Murphy, S. M.; Murphy, D. M.; de Gouw, J. A.; Eddingsaas, N. C.; Wennberg, P. O. Contribution of Isoprene-Derived Organosulfates to Free Tropospheric Aerosol Mass. *Proc. Natl. Acad. Sci.* **2010**, *107*, 21360−21365.
(41) Pratt, K. A.; Fiddler, M. N.; Shepson, P. B.; Carlton, A. G.; Surratt, J. D. Organosulfates in Cloud Water above the Ozarks' Isoprene Source Region. *Atmos. Environ* **2013**, *77*, 231−238.
(42) Cui, T.; Zeng, Z.; dos Santos, E. O.; Zhang, Z.; Chen, Y.; Zhang, Y.; Rose, C. A.; Budisulistiorini, S. H.; Collins, L. B.; Bodnar, W. M.; de Souza, R. A. F.; Martin, S. T.; Machado, C. M. D.; Turpin, B. J.; Gold, A.; Ault, A. P.; Surratt, J. D. Development of a Hydrophilic Interaction Liquid Chromatography (HILIC) Method for the Chemical Characterization of Water-Soluble Isoprene Epoxydiol (IEPOX)-Derived Secondary Organic Aerosol. *Environ. Sci. Process. Impacts* **2018**, *20*, 1524−1536.
(43) Isaacman-VanWertz, G.; Yee, L. D.; Kreisberg, N. M.; Wernis, R.; Moss, J. A.; Hering, S. V.; de Sá, S. S.; Martin, S. T.; Alexander, M. L.; Palm, B. B.; Hu, W.; Campuzano-Jost, P.; Day, D. A.; Jimenez, J. L.; Riva, M.; Surratt, J. D.; Viegas, J.; Manzi, A.; Edgerton, E.; Baumann, K.; Souza, R.; Artaxo, P.; Goldstein, A. H. Ambient Gas-Particle Partitioning of Tracers for Biogenic Oxidation. *Environ. Sci. Technol.* **2016**, *50*, 9952−9962.
(44) Lopez-Hilfiker, F. D.; Mohr, C.; D'Ambro, E. L.; Lutz, A.; Riedel, T. P.; Gaston, C. J.; Iyer, S.; Zhang, Z.; Gold, A.; Surratt, J. D.; Lee, B. H.; Kurten, T.; Hu, W. W.; Jimenez, J.; Hallquist, M.; Thornton, J. A. Molecular Composition and Volatility of Organic Aerosol in the Southeastern U . S .: Implications for IEPOX Derived SOA. *Environ. Sci. Technol.* **2016**, *50*, 2200−2209.
(45) Hu, W.; Palm, B. B.; Day, D. A.; Campuzano-Jost, P.; Krechmer, J. E.; Peng, Z.; de Sá, S. S.; Martin, S. T.; Alexander, M. L.; Baumann, K.; Hacker, L.; Kiendler-Scharr, A.; Koss, A. R.; De Gouw, J. A.; Goldstein, A. H.; Seco, R.; Sjostedt, S. J.; Park, J.-H.; Guenther, A. B.; Kim, S.; Canonaco, F.; Prévôt, A. S. H.; Brune, W. H.; Jimenez, J. L. Volatility and Lifetime against OH Heterogeneous Reaction of Ambient Isoprene-Epoxydiols-Derived Secondary Organic Aerosol (IEPOX-SOA). *Atmos. Chem. Phys.* **2016**, *16*, 11563−11580.
(46) Kroll, J. H.; Ng, N. L.; Murphy, S. M.; Flagan, R. C.; Seinfeld, J. H. Secondary Organic Aerosol Formation from Isoprene Photooxidation under High-NOx Conditions. *Geophys. Res. Lett.* **2005**, *32*, 1−4.
(47) Lin, Y.-H.; Zhang, H.; Pye, H. O. T.; Zhang, Z.; Marth, W. J.; Park, S.; Arashiro, M.; Cui, T.; Budisulistiorini, S. H.; Sexton, K. G.; Vizuete, W.; Xie, Y.; Luecken, D. J.; Piletic, I. R.; Edney, E. O.; Bartolotti, L. J.; Gold, A.; Surratt, J. D. Epoxide as a Precursor to Secondary Organic Aerosol Formation from Isoprene Photooxidation in the Presence of Nitrogen Oxides. *Proc. Natl. Acad. Sci. U. S. A.* **2013**, *110*, 6718−6723.
(48) Nguyen, T. B.; Bates, K. H.; Crounse, J. D.; Schwantes, R. H.; Zhang, X.; Kjaergaard, H. G.; Surratt, J. D.; Lin, P.; Laskin, A.; Seinfeld, J. H.; Wennberg, P. O. Mechanism of the Hydroxyl Radical Oxidation of Methacryloyl Peroxynitrate (MPAN) and Its Pathway toward Secondary Organic Aerosol Formation in the Atmosphere. *Phys. Chem. Chem. Phys.* **2015**, *17*, 17914−17926.
(49) Dommen, J.; Metzger, A.; Duplissy, J.; Kalberer, M.; Alfarra, M. R.; Gascho, A.; Weingartner, E.; Prevot, A. S. H.; Verheggen, B.; Baltensperger, U. Laboratory Observation of Oligomers in the Aerosol from Isoprene/$NO_x$ Photooxidation. *Geophys. Res. Lett.* **2006**, *33*, L13805.
(50) Szmigielski, R.; Surratt, J. D.; Vermeylen, R.; Szmigielska, K.; Kroll, J. H.; Ng, N. L.; Murphy, S. M.; Sorooshian, A.; Seinfeld, J. H.; Claeys, M. Characterization of 2-Methylglyceric Acid Oligomers in Secondary Organic Aerosol Formed from the Photooxidation of Isoprene Using Trimethylsilylation and Gas Chromatography/Ion Trap Mass Spectrometry. *J. Mass Spectrom.* **2007**, *42*, 101−116.
(51) Worton, D. R.; Surratt, J. D.; LaFranchi, B. W.; Chan, A. W. H.; Zhao, Y.; Weber, R. J.; Park, J.-H.; Gilman, J. B.; De Gouw, J.; Park, C.; Schade, G.; Beaver, M.; St. Clair, J. M.; Crounse, J.; Wennberg, P.; Wolfe, G. M.; Harrold, S.; Thornton, J. A.; Farmer, D. K.; Docherty, K. S.; Cubison, M. J.; Jimenez, J.-L.; Frossard, A. A.; Russell, L. M.; Kristensen, K.; Glasius, M.; Mao, J.; Ren, X.; Brune, B.; Browne, E. C.; Pusede, S. E.; Cohen, R. C.; Seinfeld, J. H.; Goldstein, A. H. Observational Insights into Aerosol Formation from Isoprene. *Environ. Sci. Technol.* **2013**, *47*, 11403−11413.
(52) Carlton, A. G.; de Gouw, J.; Jimenez, J. L.; Ambrose, J. L.; Attwood, A. R.; Brown, S.; Baker, K. R.; Brock, C.; Cohen, R. C.; Edgerton, S.; Farkas, C. M.; Farmer, D.; Goldstein, A. H.; Gratz, L.; Guenther, A.; Hunt, S.; Jaeglé, L.; Jaffe, D. A.; Mak, J.; McClure, C.; Nenes, A.; Nguyen, T. K.; Pierce, J. R.; de Sá, S.; Selin, N. E.; Shah, V.; Shaw, S.; Shepson, P. B.; Song, S.; Stutz, J.; Surratt, J. D.; Turpin, B. J.; Warneke, C.; Washenfelder, R. A.; Wennberg, P. O.; Zhou, X. Synthesis of the Southeast Atmosphere Studies. *Bull. Am. Metorological Soc* **2018**, 547−567.
(53) Martin, S. T.; Artaxo, P.; Machado, L. A. T.; Manzi, A. O.; Souza, R. A. F.; Schumacher, C.; Wang, J.; Andreae, M. O.; Barbosa, H. M. J.; Fan, J.; Fisch, G.; Goldstein, A. H.; Guenther, A.; Jimenez, J. L.; Pöschl, U.; Silva Dias, M. A.; Smith, J. N.; Wendisch, M. Introduction: Observations and Modeling of the Green Ocean Amazon (GoAmazon2014/5). *Atmos. Chem. Phys.* **2016**, *16*, 4785−4797.
(54) Martin, S. T.; Artaxo, P.; Machado, L. A. T.; Manzi, A. O.; Souza, R. A. F.; Schumacher, C.; Wang, J.; Biscaro, T.; Brito, J.; Calheiros, A.; Jardine, K. J.; Medeiros, A.; Portela, B.; de Sá, S. S.; Adachi, K.; Aiken, A. C.; Albrecht, R.; Alexander, L.; Andreae, M. O.; Barbosa, H. M. J.; Buseck, P.; Chand, D.; Comstock, J. M.; Day, D. A.; Dubey, M.; Fan, J.; Fast, J.; Fisch, G.; Fortner, E.; Giangrande, S.; Gilles, M.; Goldstein, A. H.; Guenther, A.; Hubbe, J.; Jensen, M.; Jimenez, J. L.; Keutsch, F. N.; Kim, S.; Kuang, C.; Laskin, A.; McKinney, K.; Mei, F.; Miller, M.; Nascimento, R.; Pauliquevis, T.; Pekour, M.; Peres, J.; Petäjä, T.; Pöhlker, C.; Pöschl, U.; Rizzo, L.; Schmid, B.; Shilling, J. E.; Dias, M. A. S.; Smith, J. N.; Tomlinson, J. M.; Tóta, J.; Wendisch, M. The Green Ocean Amazon Experiment (GoAmazon2014/5) Observes Pollution Affecting Gases, Aerosols, Clouds, and Rainfall over the Rain Forest. *Bull. Am. Meteorol. Soc.* **2017**, *98*, 981−997.
(55) de Sá, S. S.; Rizzo, L. V.; Palm, B. B.; Campuzano-Jost, P.; Day, D. A.; Yee, L. D.; Wernis, R.; Isaacman-VanWertz, G.; Brito, J.; Carbone, S.; Liu, Y. J.; Sedlacek, A.; Springston, S.; Goldstein, A. H.; Barbosa, H. M. J.; Alexander, M. L.; Artaxo, P.; Jimenez, J. L.; Martin, S. T. Contributions of Biomass-Burning, Urban, and Biogenic Emissions to the Concentrations and Light-Absorbing Properties of Particulate Matter in Central Amazonia during the Dry Season. *Atmos. Chem. Phys.* **2019**, *19*, 7973−8001.
(56) Isaacman, G.; Kreisberg, N. M.; Yee, L. D.; Worton, D. R.; Chan, A. W. H.; Moss, J. A.; Hering, S. V.; Goldstein, A. H. Online


https://dx.doi.org/10.1021/acs.est.0c00805
*Environ. Sci. Technol.* 2020, 54, 5980−5991

Derivatization for Hourly Measurements of Gas- and Particle-Phase Semi-Volatile Oxygenated Organic Compounds by Thermal Desorption Aerosol Gas Chromatography (SV-TAG). *Atmos. Meas. Tech.* **2014**, *7*, 4417−4429.
(57) Yee, L. D.; Isaacman-Vanwertz, G.; Wernis, R. A.; Meng, M.; Rivera, V.; Kreisberg, N. M.; Hering, S. V.; Bering, M. S.; Glasius, M.; Upshur, M. A.; Bé, A. G.; Thomson, R. J.; Geiger, F. M.; Offenberg, J. H.; Lewandowski, M.; Kourtchev, I.; Kalberer, M.; de Sá, S. S.; Martin, S. T.; Alexander, M. L.; Palm, B. B.; Hu, W.; Campuzano-Jost, P.; Day, D. A.; Jimenez, J. L.; Liu, Y. J.; Mckinney, K. A.; Artaxo, P.; Viegas, J.; Manzi, A.; Oliveira, M. B.; De Souza, R.; Machado, L. A. T.; Longo, K.; Goldstein, A. H. Observations of Sesquiterpenes and Their Oxidation Products in Central Amazonia during the Wet and Dry Seasons. *Atmos. Chem. Phys.* **2018**, *18*, 10433−10457.
(58) Hu, W. W.; Campuzano-Jost, P.; Palm, B. B.; Day, D. A.; Ortega, A. M.; Hayes, P. L.; Krechmer, J. E.; Chen, Q.; Kuwata, M.; Liu, Y. J.; de Sá, S. S.; McKinney, K.; Martin, S. T.; Hu, M.; Budisulistiorini, S. H.; Riva, M.; Surratt, J. D.; St. Clair, J. M.; Isaacman-VanWertz, G.; Yee, L. D.; Goldstein, A. H.; Carbone, S.; Brito, J.; Artaxo, P.; De Gouw, J. A.; Koss, A.; Wisthaler, A.; Mikoviny, T.; Karl, T.; Kaser, L.; Jud, W.; Hansel, A.; Docherty, K. S.; Alexander, M. L.; Robinson, N. H.; Coe, H.; Allan, J. D.; Canagaratna, M. R.; Paulot, F.; Jimenez, J. L. Characterization of a Real-Time Tracer for Isoprene Epoxydiols-Derived Secondary Organic Aerosol (IEPOX-SOA) from Aerosol Mass Spectrometer Measurements. *Atmos. Chem. Phys.* **2015**, *15*, 11807−11833.
(59) de Sá, S. S.; Palm, B. B.; Campuzano-Jost, P.; Day, D. A.; Hu, W.; Isaacman-VanWertz, G.; Yee, L. D.; Brito, J.; Carbone, S.; Ribeiro, I. O.; Cirino, G. G.; Liu, Y.; Thalman, R.; Sedlacek, A.; Funk, A.; Schumacher, C.; Shilling, J.; Schneider, J.; Artaxo, P.; Goldstein, A. H.; Souza, R. A. F.; Wang, J.; McKinney, K. A.; Barbosa, H.; Lizabeth Alexander, M.; Jimenez, J. L.; Martin, S. T. Urban Influence on the Concentration and Composition of Submicron Particulate Matter in Central Amazonia. *Atmos. Chem. Phys.* **2018**, *18*, 12185−12206.
(60) Riva, M.; Budisulistiorini, S. H.; Zhang, Z.; Gold, A.; Surratt, J. D. Chemical Characterization of Secondary Organic Aerosol Constituents from Isoprene Ozonolysis in the Presence of Acidic Aerosol. *Atmos. Environ.* **2016**, *130*, 5−13.
(61) Glasius, M.; Bering, M. S.; Yee, L. D.; De Sá, S. S.; Isaacman-Vanwertz, G.; Wernis, R. A.; Barbosa, H. M. J.; Alexander, M. L.; Palm, B. B.; Hu, W.; Campuzano-Jost, P.; Day, D. A.; Jimenez, J. L.; Shrivastava, M.; Martin, S. T.; Goldstein, A. H. Organosulfates in Aerosols Downwind of an Urban Region in Central Amazon. *Environ. Sci. Process. Impacts* **2018**, *20*, 1546−1558.
(62) Su, L.; Patton, E. G.; Vilà-Guerau De Arellano, J.; Guenther, A. B.; Kaser, L.; Yuan, B.; Xiong, F.; Shepson, P. B.; Zhang, L.; Miller, D. O.; Brune, W. H.; Baumann, K.; Edgerton, E.; Weinheimer, A.; Misztal, P. K.; Park, J.-H.; Goldstein, A. H.; Skog, K. M.; Keutsch, F. N.; Mak, J. E. Understanding Isoprene Photooxidation Using Observations and Modeling over a Subtropical Forest in the Southeastern US. *Atmos. Chem. Phys.* **2016**, *16*, 7725−7741.
(63) Liu, Y.; Brito, J.; Dorris, M. R.; Rivera-Rios, J. C.; Seco, R.; Bates, K. H.; Artaxo, P.; Duvoisin, S., Jr.; Keutsch, F. N.; Kim, S.; Goldstein, A. H.; Guenther, A. B.; Manzi, A. O.; Souza, R. A. F.; Springston, S. R.; Watson, T. B.; McKinney, K. A.; Martin, S. T. Isoprene Photochemistry over the Amazon Rainforest. *Proc. Natl. Acad. Sci.* **2016**, *113*, 6125−6130.
(64) Fountoukis, C.; Nenes, A. *Atmospheric Chemistry and Physics ISORROPIA II: A Computationally Efficient Thermodynamic Equilibrium Model for K +-Ca 2+-Mg 2+-NH + 4-Na +-SO 2−4-NO − 3-Cl −-H 2 O Aerosols*; 2007; Vol. 7.
(65) Hansen, D. A.; Edgerton, E. S.; Hartsell, B. E.; Jansen, J. J.; Kandasamy, N.; Hidy, G. M.; Blanchard, C. L. The Southeastern Aerosol Research and Characterization Study: Part 1-Overview. *J. Air Waste Manage. Assoc.* **2012**, *53*, 1460−1471.
(66) Mather, J. H.; Voyles, J. W. The Arm Climate Research Facility: A Review of Structure and Capabilities. *Bull. Am. Meteorol. Soc.* **2013**, *94*, 377−392.
(67) Liu, Y.; Seco, R.; Kim, S.; Guenther, A. B.; Goldstein, A. H.; Keutsch, F. N.; Springston, S. R.; Watson, T. B.; Artaxo, P.; Souza, R. A. F.; McKinney, K. A.; Martin, S. T. Isoprene Photo-Oxidation Products Quantify the Effect of Pollution on Hydroxyl Radicals over Amazonia. *Sci. Adv* **2018**, *4*, eaar2547.
(68) Hidy, G. M.; Blanchard, C. L.; Baumann, K.; Edgerton, E.; Tanenbaum, S.; Shaw, S.; Knipping, E.; Tombach, I.; Jansen, J.; Walters, J. Chemical Climatology of the Southeastern United States, 1999−2013. *Atmos. Chem. Phys.* **2014**, *14*, 11893−11914.
(69) Xu, L.; Middlebrook, A. M.; Liao, J.; de Gouw, J. A.; Guo, H.; Weber, R. J.; Nenes, A.; Lopez-Hilfiker, F. D.; Lee, B. H.; Thornton, J. A.; Brock, C. A.; Neuman, J. A.; Nowak, J. B.; Pollack, I. B.; Welti, A.; Graus, M.; Warneke, C.; Ng, N. L. Enhanced Formation of Isoprene-Derived Organic Aerosol in Sulfur-Rich Power Plant Plumes during Southeast Nexus. *J. Geophys. Res. Atmos.* **2016**, *121*, 11,137−11,153.
(70) Eddingsaas, N. C.; VanderVelde, D. G.; Wennberg, P. O. Kinetics and Products of the Acid-Catalyzed Ring-Opening of Atmospherically Relevant Butyl Epoxy Alcohols. *J. Phys. Chem. A* **2010**, *114*, 8106−8113.
(71) Riva, M.; Bell, D. M.; Hansen, A.-M. K.; Drozd, G. T.; Zhang, Z.; Gold, A.; Imre, D.; Surratt, J. D.; Glasius, M.; Zelenyuk, A. Effect of Organic Coatings, Humidity and Aerosol Acidity on Multiphase Chemistry of Isoprene Epoxydiols. *Environ. Sci. Technol.* **2016**, *50*, 5580−5588.
(72) Li, J.; Wang, G.; Wu, C.; Cao, C.; Ren, Y.; Wang, J.; Li, J.; Cao, J.; Zeng, L.; Zhu, T. Characterization of Isoprene-Derived Secondary Organic Aerosols at a Rural Site in North China Plain with Implications for Anthropogenic Pollution Effects. *Nature* **2018**, *8*, 535−510.
(73) Andreae, M. O.; Berresheim, H.; Bingemer, H.; Jacob, D. J.; Lewis, B. L.; Li, S.-M.; Talbot, R. W. The Atmospheric Sulfur Cycle over the Amazon Basin: 2. Wet Season. *J. Geophys. Res.* **1990**, *95*, 16813.
(74) Chen, Q.; Farmer, D. K.; Schneider, J.; Zorn, S. R.; Heald, C. L.; Karl, T. G.; Guenther, A.; Allan, J. D.; Robinson, N.; Coe, H.; Kimmel, J. R.; Pauliquevis, T.; Borrmann, S.; Pöschl, U.; Andreae, M. O.; Artaxo, P.; Jimenez, J. L.; Martin, S. T. Mass Spectral Characterization of Submicron Biogenic Organic Particles in the Amazon Basin. *Geophys. Res. Lett.* **2009**, *36*, L20806.
(75) Martin, S. T.; Andreae, M. O.; Artaxo, P.; Baumgardner, D.; Chen, Q.; Goldstein, A. H.; Guenther, A.; Heald, C. L.; Mayol-Bracero, O. L.; McMurry, P. H.; Pauliquevis, T.; Pöschl, U.; Prather, K. A.; Roberts, G. C.; Saleska, S. R.; Silva Dias, M. A.; Spracklen, D. V.; Swietlicki, E.; Trebs, I. Sources and Properties of Amazonian Aerosol Particles. *Rev. Geophys.* **2010**, *48*, RG2002.
(76) Tolocka, M. P.; Turpin, B. Contribution of Organosulfur Compounds to Organic Aerosol Mass. *Environ. Sci. Technol.* **2012**, *46*, 7978−7983.
(77) Hansen, A.-M. K.; Kristensen, K.; Nguyen, Q. T.; Zare, A.; Cozzi, F.; Nøjgaard, J. K.; Skov, H.; Brandt, J.; Christensen, J. H.; Ström, J.; Tunved, P.; Krejci, R.; Glasius, M. Organosulfates and Organic Acids in Arctic Aerosols: Speciation, Annual Variation and Concentration Levels. *Atmos. Chem. Phys.* **2014**, *14*, 7807−7823.
(78) Kourtchev, I.; Doussin, J.-F.; Giorio, C.; Mahon, B.; Wilson, E. M.; Maurin, N.; Pangui, E.; Venables, D. S.; Wenger, J. C.; Kalberer, M. Molecular Composition of Fresh and Aged Secondary Organic Aerosol from a Mixture of Biogenic Volatile Compounds: A High-Resolution Mass Spectrometry Study. *Atmos. Chem. Phys.* **2015**, *15*, 5683−5695.
(79) Kjaergaard, H. G.; Knap, H. C.; Ørnsø, K. B.; Jørgensen, S.; Crounse, J. D.; Paulot, F.; Wennberg, P. O. Atmospheric Fate of Methacrolein. 2. Formation of Lactone and Implications for Organic Aerosol Production. *J. Phys. Chem. A* **2012**, *116*, 5763−5768.
(80) Kuwata, M.; Liu, Y.; Mckinney, K.; Martin, S. T. Physical State and Acidity of Inorganic Sulfate Can Regulate the Production of Secondary Organic Material from Isoprene Photooxidation Products. *Phys. Chem. Chem. Phys.* **2015**, *17*, 5670.
(81) Blanchard, C. L.; Hidy, G. M.; Shaw, S.; Baumann, K.; Edgerton, E. S. Effects of Emission Reductions on Organic Aerosol in


https://dx.doi.org/10.1021/acs.est.0c00805
*Environ. Sci. Technol.* 2020, 54, 5980−5991

the Southeastern United States. *Atmos. Chem. Phys.* **2016**, *16*, 215−238.
(82) Jardine, K.; Yañez-Serrano, A. M.; Williams, J.; Kunert, N.; Jardine, A.; Taylor, T.; Abrell, L.; Artaxo, P.; Guenther, A.; Hewitt, C. N.; House, E.; Florentino, A. P.; Manzi, A.; Higuchi, N.; Kesselmeier, J.; Behrendt, T.; Veres, P. R.; Derstroff, B.; Fuentes, J. D.; Martin, S. T.; Andreae, M. O. Dimethyl Sulfide in the Amazon Rain Forest. *Global Biogeochem. Cycles* **2015**, *29*, 19−32.
(83) Saturno, J.; Ditas, F.; Penning De Vries, M.; Holanda, B. A.; Pöhlker, M. L.; Carbone, S.; Walter, D.; Bobrowski, N.; Brito, J.; Chi, X.; Gutmann, A.; Hrabe De Angelis, I.; Machado, L. A. T.; Moran-Zuloaga, D.; Rüdiger, J.; Schneider, J.; Schulz, C.; Wang, Q.; Wendisch, M.; Artaxo, P.; Wagner, T.; Pöschl, U.; Andreae, M. O.; Pöhlker, C. African Volcanic Emissions Influencing Atmospheric Aerosols over the Amazon Rain Forest. *Atmos. Chem. Phys.* **2018**, *18*, 10391−10405.
(84) Andreae, M. O.; Merlet, P. Emission of Trace Gases and Aerosols from Biomass Burning. *Global Biogeochem. Cycles* **2001**, *15*, 955−966.
(85) Hand, J. L.; Schichtel, B. A.; Malm, W. C.; Pitchford, M. L. Particulate Sulfate Ion Concentration and $SO_2$ Emission Trends in the United States from the Early 1990s through 2010. *Atmos. Chem. Phys.* **2012**, *12*, 10353−10365.
(86) Estillore, A. D.; Hettiyadura, A. P. S.; Qin, Z.; Leckrone, E.; Wombacher, B.; Humphry, T.; Stone, E. A.; Grassian, V. H. Water Uptake and Hygroscopic Growth of Organosulfate Aerosol. *Environ. Sci. Technol.* **2016**, *50*, 4259−4268.
(87) Vogel, A. L.; Schneider, J.; Müller-Tautges, C.; Phillips, G. J.; Pöhlker, M. L.; Rose, D.; Zuth, C.; Makkonen, U.; Hakola, H.; Crowley, J. N.; Andreae, M. O.; Pöschl, U.; Hoffmann, T. Aerosol Chemistry Resolved by Mass Spectrometry: Linking Field Measurements of Cloud Condensation Nuclei Activity to Organic Aerosol Composition. *Environ. Sci. Technol.* **2016**, *50*, 10823−10832.
(88) Zhang, H.; Lin, Y.-H.; Zhang, Z.; Zhang, X.; Shaw, S. L.; Knipping, E. M.; Weber, R. J.; Gold, A.; Kamens, R. M.; Surratt, J. D. Secondary Organic Aerosol Formation from Methacrolein Photooxidation: Roles of NOx Level, Relative Humidity and Aerosol Acidity. *Environ. Chem.* **2012**, *9*, 247−262.
(89) Tanner, R. L.; Olszyna, K. J.; Edgerton, E. S.; Knipping, E.; Shaw, S. L. Searching for Evidence of Acid-Catalyzed Enhancement of Secondary Organic Aerosol Formation Using Ambient Aerosol Data. *Atmos. Environ.* **2009**, *43*, 3440−3444.
(90) Jang, M.; Czoschke, N. M.; Lee, S.; Kamens, R. M. Heterogeneous Atmospheric Aerosol Production by Acid-Catalyzed Particle-Phase Reactions. *Science* **2002**, *298*, 814−817.
(91) Weber, R. J.; Guo, H.; Russell, A. G.; Nenes, A. High Aerosol Acidity despite Declining Atmospheric Sulfate Concentrations over the Past 15 Years. *Nat. Geosci.* **2016**, *9*, 282.
(92) D'Ambro, E. L.; Schobesberger, S.; Gaston, C. J.; Lopez-Hilfiker, F. D.; Lee, B. H.; Liu, J.; Zelenyuk, A.; Bell, D.; Cappa, C. D.; Helgestad, T.; Li, Z.; Guenther, A.; Wang, J.; Wise, M.; Caylor, R.; Surratt, J. D.; Riedel, T.; Hyttinen, N.; Salo, V.-T.; Hasan, G.; Kurten, T.; Shilling, J. E.; Thornton, J. A. Chamber-Based Insights into the Factors Controlling Epoxydiol (IEPOX) Secondary Organic Aerosol (SOA) Yield, Composition, and Volatility. *Atmos. Chem. Phys.* **2019**, *19*, 11253−11265.
(93) Kleindienst, T. E.; Lewandowski, M.; Offenberg, J. H.; Jaoui, M.; Edney, E. O. Ozone-Isoprene Reaction : Re-Examination of the Formation of Secondary Organic Aerosol. *Geophys. Res. Lett.* **2007**, *34*, 1−6.
(94) Bateman, A. P.; Gong, Z.; Liu, P.; Sato, B.; Cirino, G.; Zhang, Y.; Artaxo, P.; Bertram, A. K.; Manzi, A. O.; Rizzo, L. V.; Souza, R. A. F.; Zaveri, R. A.; Martin, S. T. Sub-Micrometre Particulate Matter Is Primarily in Liquid Form over Amazon Rainforest. *Nat. Geosci.* **2016**, *9*, 34−37.
(95) Pajunoja, A.; Hu, W.; Leong, Y. J.; Taylor, N. F.; Miettinen, P.; Palm, B. B.; Mikkonen, S.; Collins, D. R.; Jimenez, J. L.; Virtanen, A. Phase State of Ambient Aerosol Linked with Water Uptake and Chemical Aging in the Southeastern US. *Atmos. Chem. Phys.* **2016**, *16*, 11163−11176.


https://dx.doi.org/10.1021/acs.est.0c00805
*Environ. Sci. Technol.* 2020, 54, 5980−5991